

## Accepted Manuscript

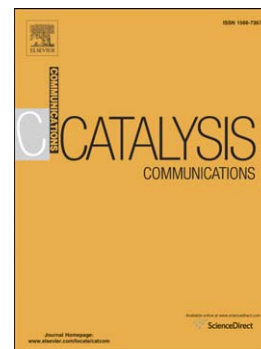
Novel Ni<sub>2</sub>P/Zeolite Catalysts for Naphthalene Hydrocracking to BTX

Yong-Su Kim, Gwang-Nam Yun, Yong-Kul Lee

PII: S1566-7367(13)00437-8  
DOI: doi: [10.1016/j.catcom.2013.11.010](https://doi.org/10.1016/j.catcom.2013.11.010)  
Reference: CATCOM 3713

To appear in: *Catalysis Communications*

Received date: 23 August 2013  
Revised date: 7 October 2013  
Accepted date: 8 November 2013



Please cite this article as: Yong-Su Kim, Gwang-Nam Yun, Yong-Kul Lee, Novel Ni<sub>2</sub>P/Zeolite Catalysts for Naphthalene Hydrocracking to BTX, *Catalysis Communications* (2013), doi: [10.1016/j.catcom.2013.11.010](https://doi.org/10.1016/j.catcom.2013.11.010)

This is a PDF file of an unedited manuscript that has been accepted for publication. As a service to our customers we are providing this early version of the manuscript. The manuscript will undergo copyediting, typesetting, and review of the resulting proof before it is published in its final form. Please note that during the production process errors may be discovered which could affect the content, and all legal disclaimers that apply to the journal pertain.

Novel Ni<sub>2</sub>P/Zeolite Catalysts for Naphthalene Hydrocracking to BTX

Yong-Su Kim, Gwang-Nam Yun, and Yong-Kul Lee\*

Laboratory of Advanced Catalysis for Energy and Environment,  
Department of Chemical Engineering, Dankook University,  
126 Jukjeondong, Yongin 448-701, South Korea

\*To whom all correspondence should be addressed. Email: yolee@dankook.ac.kr

## Abstract

Ni<sub>2</sub>P catalysts supported on ZSM-5, Beta, and USY zeolites were prepared by temperature-programmed reduction (TPR), applied for the hydrocracking of naphthalene, and characterized by BET, CO uptake, NH<sub>3</sub>-TPD, TEM, X-ray diffraction (XRD), and extended X-ray absorption fine structure (EXAFS). The catalytic activity was tested at 673 K and 3.0 MPa in a three-phase fixed bed reactor for hydrocracking of naphthalene. The Ni<sub>2</sub>P/Beta exhibited best activity with a naphthalene conversion of 99%, and a BTX yield of 94.4%. Well-dispersed Ni<sub>2</sub>P particles combined with moderate acidity and porosity of zeolite Beta contributed to the enhanced hydrocracking activity of naphthalene into BTX.

Keywords: Ni<sub>2</sub>P/Beta, Hydrocracking, Naphthalene, BTX, EXAFS

## 1. Introduction

Polyaromatic hydrocarbon compounds (PAH) of naphthalene, anthracene and phenanthrene are highly required to upgrade into lighter oil fractions such as benzene, toluene and xylene (BTX) [1-2]. Catalytic hydrocracking is the most effective option to break up the PAHs into BTX over bifunctional catalysts via hydrogenation and cracking [3-5]. Accordingly, partial hydrogenation of the polyaromatic rings and cracking of the resulting naphthenic rings are key steps in the hydrocracking reaction, so that bifunctional catalysts such as metals supported on acid catalysts have mostly been applied [5-9]. In this regard, the effect of metal catalysts on the hydrocracking of two or three-ring aromatic compounds and alkyl aromatic compounds has been investigated by a number of investigators [4-5, 10-13]. According to the previous studies, transition or noble metal catalysts such as Mo, W, Co-Mo, Ni-Mo, Ni-W, Pt, or Pt-Pd metals supported on  $\text{SiO}_2\text{-Al}_2\text{O}_3$  or zeolites have been adopted for the hydrocracking at relatively high temperatures around 773-1073 K and at high  $\text{H}_2$  pressures 8-15 MPa, however, the BTX yield, less than 50% in most cases, should be enhanced for the commercial application.

A new hydroprocessing catalyst group of transition metal phosphides has recently been introduced [14-17]. Among the transition metal phosphide catalysts,  $\text{Ni}_2\text{P}$  catalyst is known to show best activity in hydrotreating [15-17]. Moreover, the  $\text{Ni}_2\text{P}$  catalysts have shown superior hydrogenation activity, even under the presence of nitrogen compounds [17-19]. In the present study, we have thus applied  $\text{Ni}_2\text{P}$  catalysts supported on various zeolites to examine the effect of acidity and porosity of different types of zeolite supports on the bifunctional catalytic activity for naphthalene hydrocracking into BTX.

## 2. Experimental

The supports used in this study were Zeolite Beta (CP814E, Zeolyst), USY(CBV780, Zeolyst), ZSM-5(CBV3024E, Zeolyst), and SiO<sub>2</sub>(Cab-O-Sil M5, Cabot). Supported Ni<sub>2</sub>P catalysts were prepared by incipient wetness impregnation of aqueous metal phosphate precursors, followed by temperature programmed reduction (TPR) in flowing hydrogen. The initial Ni/P ratio in the precursors was fixed at 1/2. The amount of Ni loading was fixed at 1.5 mmol/g of support. The supported nickel phosphate precursor was prepared by incipient wetness impregnation of a solution of nickel nitrate Ni(NO<sub>3</sub>)<sub>2</sub>·6H<sub>2</sub>O (Alfa Aesar, 98 %) and ammonium phosphate (NH<sub>4</sub>)<sub>2</sub>HPO<sub>4</sub> (Samchun, 99 %), followed by drying at 393 K for 7 h and calcination at 673 K for 4 h.

The resulting precursor phosphates were reduced to the corresponding phosphides by TPR from 298 to 873 K (at 5 Kmin<sup>-1</sup>). The prepared catalysts were characterized by X-ray diffraction (XRD), N<sub>2</sub> adsorption, CO chemisorption, temperature programmed desorption of NH<sub>3</sub> (NH<sub>3</sub>-TPD), and HR-TEM. Also, X-ray absorption spectroscopy (XAS) at the Ni K edge (8.333 keV) of reference and catalyst samples was carried out in the energy range 8.233 to 9.283 keV at the beamline 8C of the Pohang Light Source (PLS).

Hydrocracking was carried out at 3.0MPa and 673K in a continuous-flow reactor using a model feed mixture containing aromatic and aliphatic compounds. The feed liquid was prepared by combining 5 wt% naphthalene (Aldrich, 99%) in tridecane (TCI, 99%). The liquid mixture was delivered at 0.05 cm<sup>3</sup> min<sup>-1</sup> using a liquid pump (Laballiance series II) along with 100 cm<sup>3</sup> min<sup>-1</sup> of hydrogen flow. Quantities of catalysts loaded in the reactor were 1.0 cm<sup>3</sup> for the Ni<sub>2</sub>P catalysts with corresponding liquid hourly space velocity (LHSV) of 3.0 h<sup>-1</sup>. Liquid product

compositions were determined with a Hewlett Packard 5890A gas chromatograph, equipped with a 60 m dimethylsiloxane column having 0.32 mm i.d. (Hewlett Packard, HP-1), on samples collected at 3 to 4 h intervals. The conversion of naphthalene was calculated using Eq. (1) where  $NAPH_{initial}$  and  $NAPH_{final}$  were moles of naphthalene before and after the reaction, respectively. The yield of BTX was calculated using Eq. (2) from the moles of naphthalene in feed and BTX in product. Tridecane also underwent hydrocracking to give lower aliphatic species C5, C6, and C7 of 95wt% and gaseous species of C2 and C3 of less than 5wt %. Carbon balance confirmed that the alkylation from the solvent fragments was negligible and BTX formation was fully dependent upon the hydrocracking of naphthalene.

$$Naphthalene\ conversion\ (\%) = \frac{NAPH_{initial} - NAPH_{final}}{NAPH_{initial}} \times 100 \quad (1)$$

$$BTX\ yield\ (\%) = \frac{Benzene + Toluene + Xylenes}{NAPH_{initial}} \times 100 \quad (2)$$

### 3. Results and Discussion

Table 1 summarizes the physical properties of the zeolite supports and catalyst samples. As for the zeolite supports, the surface area followed the order USY>Beta>ZSM-5. It was observed that Beta and USY retained mesoporosity, originated from inter-particulate pore system in Beta and intra-crystalline mesoporous feature in USY, as also reported in previous studies [18-21]. It can be seen that the BET surface area of supported Ni<sub>2</sub>P catalyst samples decreased due to a reduction in the pore volume with the loadings of Ni<sub>2</sub>P. The spent samples exhibited a partial reduction in the surface area due to the retention of reaction products on the catalysts.

Chemisorption quantities of CO were reported to correlate closely with dispersion of Ni<sub>2</sub>P

catalyst since CO species could effectively titrate active centers of Ni<sub>2</sub>P via the formation of  $\pi$  back-bonding of higher-electron density Ni species [19]. The amount of CO uptake for the catalyst samples followed the order Ni<sub>2</sub>P/USY > Ni<sub>2</sub>P/Beta > Ni<sub>2</sub>P/ZSM-5 > Ni<sub>2</sub>P/SiO<sub>2</sub>, with a significant reduction in CO uptake amount being observed for Ni<sub>2</sub>P/ZSM-5, indicating the loss of active sites, probably due to the agglomeration of Ni<sub>2</sub>P particles or coke deposition in the course of reaction. Table 1 also lists the elemental analysis results of the molar ratios of P/Ni in the fresh and spent Ni<sub>2</sub>P samples, as determined by ICP-AES. Although the samples were prepared with an initial P/Ni ratio of 2/1, the freshly prepared samples were found to contain lower phosphorus amounts than the initial value, with P/Ni ratios ranging from 0.8 to 2.0. A previous work has shown that phosphorus is removed as PH<sub>3</sub> during the reduction procedure [17]. After reaction, the samples underwent further loss in P to give reduced P/Ni ratios, ranging from 0.59 to 1.50 closed to the stoichiometric value of 0.5 for Ni<sub>2</sub>P.

Figure 1 shows the powder XRD patterns of the fresh and spent Ni<sub>2</sub>P catalysts, as well as a Ni<sub>2</sub>P reference. The diffraction pattern for Ni<sub>2</sub>P shows three main peaks at 40.5°, 44.8° and 47.5° corresponding to lattice planes (111), (201), and (210) of Ni<sub>2</sub>P. The XRD patterns confirm that a Ni<sub>2</sub>P phase is formed on the Beta, USY, ZSM-5, and SiO<sub>2</sub> support. After reaction the peaks for zeolite and Ni<sub>2</sub>P phase were virtually retained with little changes in the peak positions.

Figure 2 shows comparison of the Ni K-edge and EXAFS spectra for the fresh and spent Ni<sub>2</sub>P catalyst and bulk Ni<sub>2</sub>P samples. The EXAFS spectrum for Ni<sub>2</sub>P comprises a little wider oscillation region in 30.0–80.0 nm<sup>-1</sup> due to Ni–P contribution and a narrower oscillation region in 80.0–140.0 nm<sup>-1</sup> due to Ni–Ni contribution, which gives rise to two distinct peaks in the Fourier transforms, centered at 0.175 nm and 0.240 nm, corresponding to Ni–P and Ni–Ni, respectively [19]. For the supported Ni<sub>2</sub>P samples there were also two main peaks located at

almost the same positions as those of the bulk Ni<sub>2</sub>P reference, indicating the presence of Ni<sub>2</sub>P phase on the Beta, USY, ZSM-5, and SiO<sub>2</sub> support. As for the spent samples almost similar EXAFS spectra were observed with only a little decrease in Ni–Ni peak intensity of Fourier transforms, indicating that the Ni<sub>2</sub>P phase is not significantly altered during the reaction. These results are well correlated with the XRD results shown in Fig. 1.

Figure 3 shows TEM micrographs of the fresh Ni<sub>2</sub>P catalyst samples. The zeolite supports showed different crystallite sizes of 20 nm for Beta, 0.2 μm for ZSM-5, and 0.5 μm for USY. Zeolite Beta (CP814E, Zeolyst) is known to consist of nano-crystallites with sizes between 15 and 20 nm, that are clustered into agglomerates of about 60-100 nm [20]. The supported Ni<sub>2</sub>P catalysts appeared to have relatively wide particle size distributions of 1 to 20 nm of Ni<sub>2</sub>P depending on the supports. The Ni<sub>2</sub>P/USY had smaller particles in the ranges of 1 to 7 nm, indicating better dispersion, as also proved by CO uptake results in Table 1. Similar results were observed in a previous study [21], in which Ni<sub>2</sub>P particles were well dispersed in K-USY supports with size ranges less than 5 nm. The Ni<sub>2</sub>P/Beta gave a little wider particle size distributions of 5 to 10 nm of Ni<sub>2</sub>P. On the other hand, the Ni<sub>2</sub>P/ZSM-5 had even larger Ni<sub>2</sub>P particles of 10-30 nm on the support. These results can be explained by the different structural properties of the zeolite supports. The USY has well developed mesopores in size ranges of 4-40 nm, which could render high dispersion of Ni<sub>2</sub>P particles [21]. Although the zeolite Beta does not have mesopores within the zeolite crystal, the mesopore volume can be developed by inter-crystalline particulate system, as also observed in a previous study [18]. In contrast, the ZSM-5 has mostly micropores on relatively large crystallites, resulting in low and unstable dispersion of Ni<sub>2</sub>P particles. These are in good accordance with CO uptake results for the fresh and spent catalysts with following the order: Ni<sub>2</sub>P/USY > Ni<sub>2</sub>P/Beta > Ni<sub>2</sub>P/ZSM-5.

Figure 4 shows the NH<sub>3</sub>-TPD profiles of the ZSM-5, USY, Beta, and SiO<sub>2</sub> supports, and the supported Ni<sub>2</sub>P catalyst samples. In a typical NH<sub>3</sub>-TPD profile of H-zeolites, peaks are generally observed in two temperatures regions. The regions below and above about 650K are referred to as low-temperature (LT) and high-temperature (HT) region, corresponding to weak and strong acid sites, respectively [22-23]. The NH<sub>3</sub>-TPD pattern for ZSM-5 gave two distinct peaks centered at 496 and 681K, and in the similar manner USY exhibited two peaks but at even higher temperatures of 623 and 803K, implying strong acidity of USY over ZSM-5. Differently from the NH<sub>3</sub>-TPD patterns for ZSM-5 and USY, Beta gave three peaks at around 496, 605, and 780K, with the two peaks at lower temperatures being overlapped [24]. Although SiO<sub>2</sub> did not give any NH<sub>3</sub> desorption, Ni<sub>2</sub>P/SiO<sub>2</sub> gave a NH<sub>3</sub> desorption peak at 489K, indicating a low acidity of the Ni<sub>2</sub>P catalyst. Oyama et al. also confirmed the weak acidity of Ni<sub>2</sub>P catalyst with pyridine-adsorbed in situ FTIR study, where the P-OH group developed on Ni<sub>2</sub>P surface exhibited a weak acidity enough to protonate pyridine [19]. As for the Ni<sub>2</sub>P/zeolites catalysts, the NH<sub>3</sub>-TPD profiles showed substantial reduction of NH<sub>3</sub> desorption particularly at high temperature region, indicating the loss of strong acid sites upon the Ni<sub>2</sub>P loadings. The loss of strong acid sites was found more pronounced for USY than the cases for Beta or ZSM-5.

Figure 5 shows the product distributions of the naphthalene hydrocracking over the Ni<sub>2</sub>P catalysts at 673K, 3.0MPa, and LHSV of 3.0 hr<sup>-1</sup>. It was found that naphthalene was well converted at the given reaction condition over the Ni<sub>2</sub>P catalysts, with following the order Ni<sub>2</sub>P/SiO<sub>2</sub> ~Ni<sub>2</sub>P/USY (90%) < Ni<sub>2</sub>P/Beta ~Ni<sub>2</sub>P/ZSM-5 (99 %), where the numbers in parenthesis indicate the conversion of naphthalene. As for the reaction products, the Ni<sub>2</sub>P/SiO<sub>2</sub> gave only hydrogenated species like tetralin and decalin with traces of BTX formation less than 0.1 %, indicating high activity in hydrogenation over hydrocracking at the reaction condition. It

was noteworthy that the zeolite-supported Ni<sub>2</sub>P catalysts showed the remarkable formation of BTX, where the BTX yield followed the order Ni<sub>2</sub>P/ZSM-5 (57.5%) < Ni<sub>2</sub>P/USY (76.4%) < Ni<sub>2</sub>P/Beta (94.4%). Considering the high activity of Ni<sub>2</sub>P for the naphthalene hydrogenation over 90% conversion in all cases, the difference in BTX yield can be more related with the nature of supports in terms of acidity and porosity. The low BTX formation together with tetralin and decalin in the product over Ni<sub>2</sub>P/ZSM-5 can be explained by the pore structure of ZSM-5 which adopts 10-MR system, smaller than 12-MR based USY or Beta, inducing a restriction of the accessibility of the hydrogenated species to the acid sites in the pore structure. As for the Ni<sub>2</sub>P/USY, the BTX formation was found a little lower than that on Ni<sub>2</sub>P/Beta, which is probably due to the lack of strong acidity and relatively larger crystallite, resulting in slow cracking activity in comparison with Ni<sub>2</sub>P/Beta catalyst.

Overall, the Ni<sub>2</sub>P plays a major role in hydrogenation of naphthalene, resulting in tetralin, and indeed the acid sites on zeolite supports function effectively in cracking the hydrogenated species into BTX. In particular, optimized acidity and pore structure of zeolite significantly promoted the bifunctional activity of Ni<sub>2</sub>P catalyst in facilitating the naphthalene hydrocracking into BTX. Therefore, it can be proposed that the Ni<sub>2</sub>P/Beta, having the unique bifunctional nature, will offer great potential in the hydrocracking of polyaromatic hydrocarbon into BTX.

#### 4. Conclusions

The hydrocracking of naphthalene into BTX has been studied over Ni<sub>2</sub>P catalysts supported on SiO<sub>2</sub>, Beta, USY, or ZSM-5. The Ni<sub>2</sub>P/SiO<sub>2</sub> catalyst was found active only for the hydrogenation of naphthalene with producing tetralin and decalin at 3.0MPa and 673K. On the other hand, the

zeolite supported Ni<sub>2</sub>P catalysts have shown remarkable activity in hydrocracking with producing BTX in the order Ni<sub>2</sub>P/Beta > Ni<sub>2</sub>P/USY > Ni<sub>2</sub>P/ZSM-5, demonstrating the bifunctional catalytic activity. The Ni<sub>2</sub>P/Beta gave the highest BTX yield of 94.4%, which was attributed to its unique catalytic nature of moderate acidity and porosity combined with hydrogenation activity of well-dispersed Ni<sub>2</sub>P phase. Moreover, the Ni<sub>2</sub>P/Beta maintained the local and bulk structure stable during the reaction as confirmed by EXAFS and XRD analysis. Overall, the Ni<sub>2</sub>P/Beta can be a potential hydrocracking catalyst for upgrading polyaromatic hydrocarbons into BTX.

## References

- [1] M. Chareonpanich, Z. G. Zhang, A. Nishijima, A. Tomita, *Fuel* 74 (1995) 1636-1640.
- [2] M. Chareonpanich, T. Boonfueng, J. Limtrakul, *Fuel Process. Technol.* 79 (2002) 171-179.
- [3] A. Ishihara, T. Itoh, H. Nasu, T. Hashimoto, T. Doi, *Fuel Process. Technol.* 116 (2013) 222-227.
- [4] J. I. Park, J. K. Lee, J. Miyawaki, Y.-K Kim, S.-H. Yoon, I. Mochida, *Fuel* 90 (2011) 182-189.
- [5] A. T. Lapinas, M. T. Klein, B. C. Gates, A. Macris, J. E. Lyons, *Ind. Eng. Chem. Res.*, 30 (1991) 42-50.
- [6] C. L. Russell, M. T. Klein, R. J. Quann, J. Trewella, *Energy Fuels* 8 (1994) 1394-1400.
- [7] A. Corma, P. J. Miguel, A.V. Orchilles, G. S. Koermer, *J. Catal.* 135 (1992) 45-59.
- [8] F. N. Guertzoni, J. Abbot, *J. Catal.* 139 (1993) 289-303.
- [9] M. Santikunaporn, J. E. Herrera, S. Jongpatiwut, D. E. Resasco, W. E. Alvarez, E. L. Sughrue, *J. Catal.* 228 (2004) 100-113.
- [10] J. L. Lemberton, M. Touzeyidio, M. Guisnet, *Appl. Catal.* 79 (1991) 115-126.
- [11] F. N. Guertzoni, J. Abbot, *J. Catal.* 139 (1993) 289-303.
- [12] H. Matsui, K. Akagi, S. Murata, M. Nomura, *Energy Fuels* 9 (1995) 435-438.
- [13] L. Leite, E. Benazzi, N. M. George, *Catal. Today* 65 (2001) 241-247.
- [14] T. I. Korányi, *Appl. Catal. A* 239 (2003) 253-267.
- [15] P. Clark, S. T. Oyama, *J. Catal.* 218 (2003) 78-87.
- [16] P. Clark, X. Wang, S. T. Oyama, *J. Catal.* 207 (2002) 256-265.
- [17] S. T. Oyama, X. Wang, Y.-K. Lee, K. Bando, F.G. Requejo, *J. Catal.* 210 (2002) 207-217.

- [18] A. N. C. van Laak, S. L. Sagala, J. Zecevic , H. Friedrich, P. E. de Jongh, K. P. de Jong, J. Catal. 276 (2010) 170–180.
- [19] Y.-K. Lee, S. T. Oyama, J. Catal. 239 (2006) 376-389.
- [20] A. N. Parvulescu, P. J. C. Hausoul, P. C. A. Bruijninx, R. J. M. K. Gebbink, B. M. Weckhuysen, Catal. Today, 158 (2010) 130–138.
- [21] Y.-K. Lee, Y. Shu, S. T. Oyama, Appl. Catal. A 322 (2007) 191-204.
- [22] M. Sawa, M. Niwa, Y. Murakami, Zeolites 10 (1990) 532-538.
- [23] H. Sato, Catal. Rev.-Sci. Eng. 39 (1997) 395-424.
- [24] F. Lonyi, J. Valyon, Thermochim. Acta 373 (2001) 53-57.

## List of Table

Table 1 Physical properties of the supports and Ni<sub>2</sub>P catalysts.

## List of Figures

Figure 1. XRD patterns of catalyst samples: (a) Ni<sub>2</sub>P/Beta - fresh, (b) Ni<sub>2</sub>P/Beta - spent, (c) Ni<sub>2</sub>P/USY -fresh, (d) Ni<sub>2</sub>P/USY - spent, (e) Ni<sub>2</sub>P/ZSM-5 - fresh, (f) Ni<sub>2</sub>P/ZSM-5 - spent, (g) Ni<sub>2</sub>P/SiO<sub>2</sub> - fresh, and (h) Ni<sub>2</sub>P/SiO<sub>2</sub> - spent.

Figure 2. Ni K-edge EXAFS spectra and Fourier transforms for fresh and spent Ni<sub>2</sub>P catalyst samples : (a) Ni<sub>2</sub>P/Beta - fresh, (b) Ni<sub>2</sub>P/Beta - spent, (c) Ni<sub>2</sub>P/USY -fresh, (d) Ni<sub>2</sub>P/USY - spent, (e) Ni<sub>2</sub>P/ZSM-5 - fresh, (f) Ni<sub>2</sub>P/ZSM-5 - spent, (g) Ni<sub>2</sub>P/SiO<sub>2</sub> - fresh and (h) Ni<sub>2</sub>P/SiO<sub>2</sub> – spent, and (i) Ni<sub>2</sub>P(bulk)

Figure 3. TEM micrographs for fresh catalyst sample : (a) Ni<sub>2</sub>P/Beta, (b) Ni<sub>2</sub>P/USY, (c) Ni<sub>2</sub>P/ZSM-5, and (d) Ni<sub>2</sub>P/SiO<sub>2</sub>

Figure 4. NH<sub>3</sub>-TPD profiles : (a) Ni<sub>2</sub>P/Beta, (b) Beta, (c) Ni<sub>2</sub>P/USY, (d) USY, (e) Ni<sub>2</sub>P/ZSM-5, (f) ZSM-5, (g) Ni<sub>2</sub>P/SiO<sub>2</sub>, and (h) SiO<sub>2</sub>

Figure 5. Activity tests for naphthalene hydrocracking at 3.0MPa, 673K, and LHSV of 3 h<sup>-1</sup> : (a) Ni<sub>2</sub>P/Beta, (b) Ni<sub>2</sub>P/USY, (c) Ni<sub>2</sub>P/ZSM-5, and (d) Ni<sub>2</sub>P/SiO<sub>2</sub>

Table 1 Physical properties of the supports and Ni<sub>2</sub>P catalysts.

Samples	Condition	BET surface area(m <sup>2</sup> g <sup>-1</sup> ) <sup>1)</sup>			Pore volume (cm <sup>3</sup> g <sup>-1</sup> )		CO uptake (μmol g <sup>-1</sup> )	Molar ratio <sup>d)</sup> P/Ni
		S <sub>total</sub>	S <sub>micro</sub> <sup>a)</sup>	S <sub>meso</sub> <sup>b)</sup>	V <sub>micro</sub> <sup>a)</sup>	V <sub>meso</sub> <sup>c)</sup>		
Beta	As calcined	60	48	12	0.	0.	-	-
		9.6	4.2	5.3	24	39		
USY		63	45	18	0.	0.	-	-
		9.6	7.6	1.9	19	24		
ZSM-5	33	28	47	0.	0.	-	-	
	3.3	5.4	.8	13	05			
SiO <sub>2</sub>	18	0.	18	0.	0.	-		
	6.3	3	5.7	01	38			
Ni <sub>2</sub> P/Beta (Si/Al = 12.5)	Fresh	40	30	10	0.	0.	2	2.0
	Spent	38	28	10	0.	0.	2	1.5
Ni <sub>2</sub> P/USY (Si/Al = 40)	Fresh	61	47	14	0.	0.	4	1.5
	Spent	56	45	10	0.	0.	3	1.3
Ni <sub>2</sub> P/ZSM-5 (Si/Al=15)	Fresh	26	21	45	0.	0.	2	1.5
	Spent	23	20	31	0.	0.	5.	1.0
Ni <sub>2</sub> P/SiO <sub>2</sub>	Fresh	12	0.	12	0.	0.	1	0.8
	Spent	74	0.	74	0.	0.	1	0.5
		.5	1	.9	01	67	3.1	

<sup>a)</sup> Calculated by *t*-plot method.

<sup>b)</sup> S<sub>total</sub> - S<sub>micro</sub>

<sup>c)</sup> V<sub>total</sub> - V<sub>micro</sub>

<sup>d)</sup> Measured by ICP elemental analysis.

Figure 1

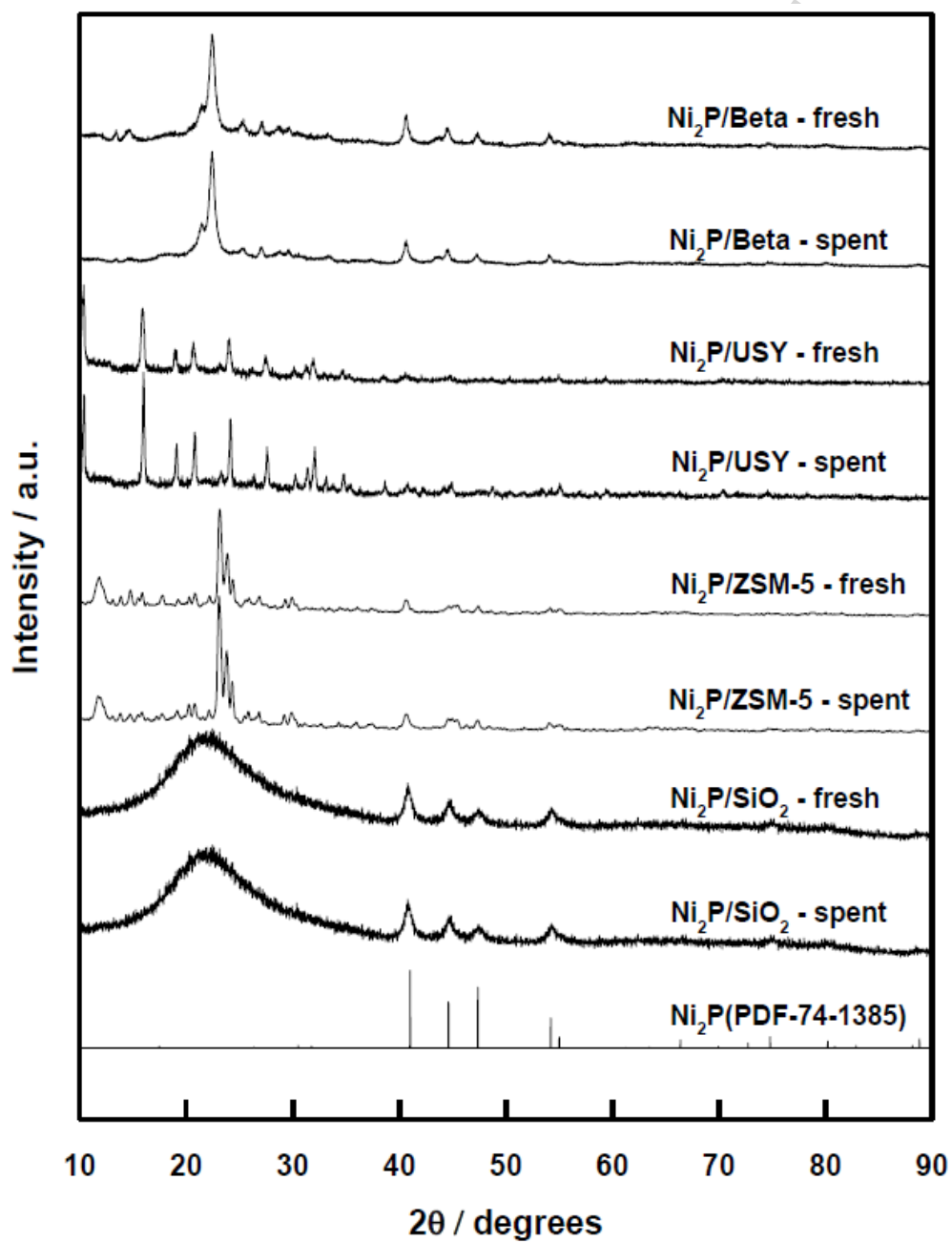
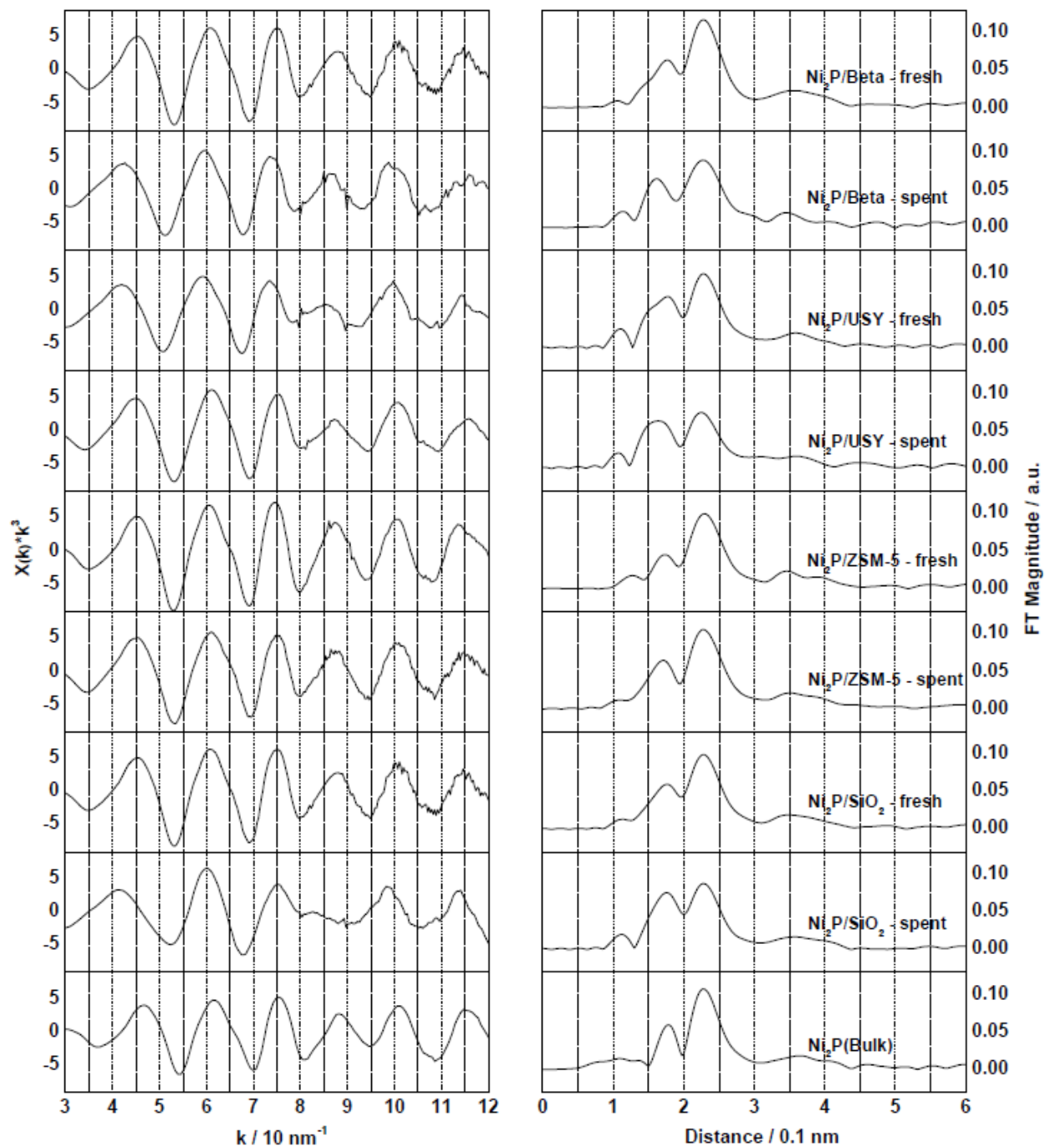


Figure 2



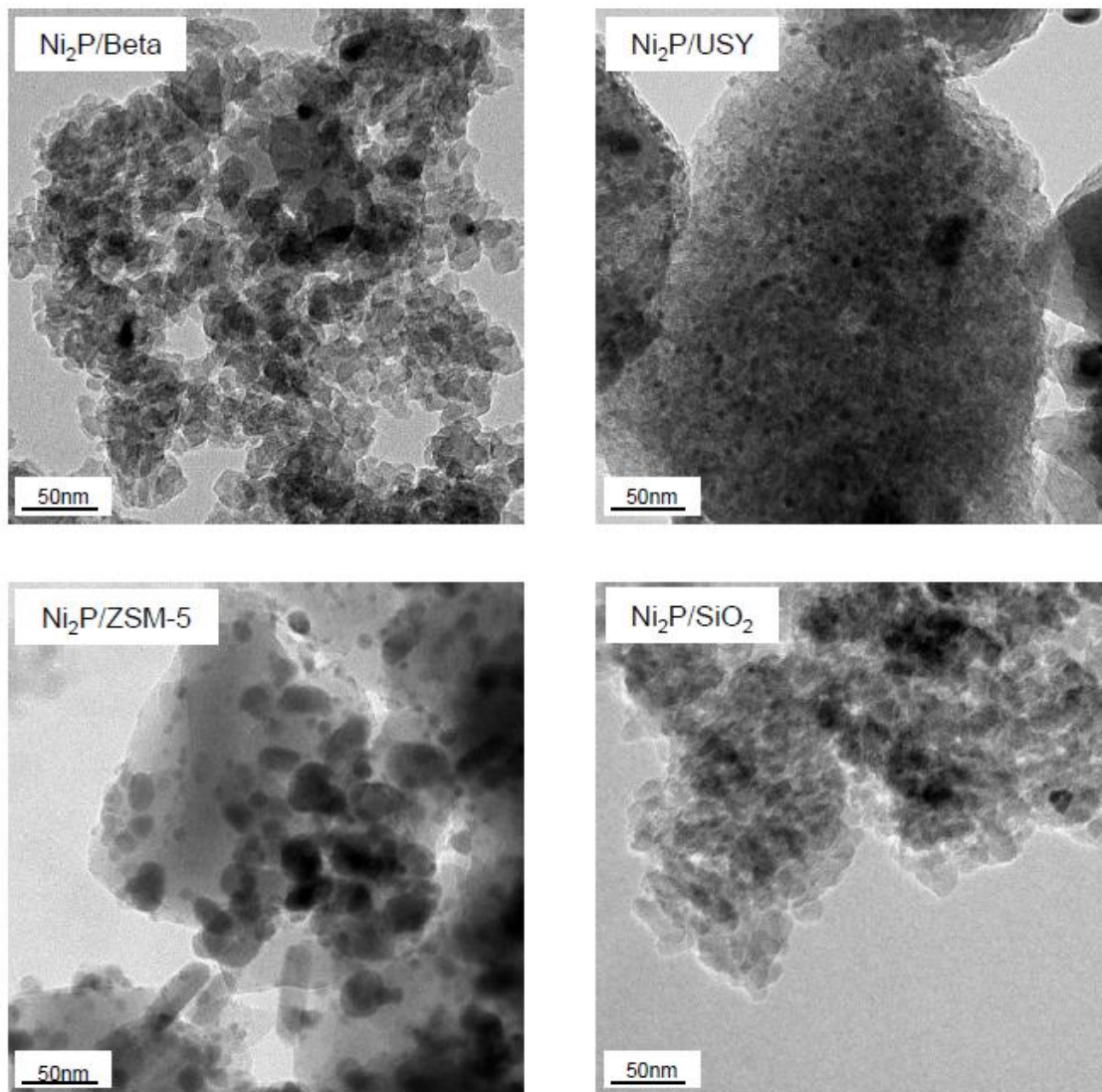
**Figure 3**

Figure 4

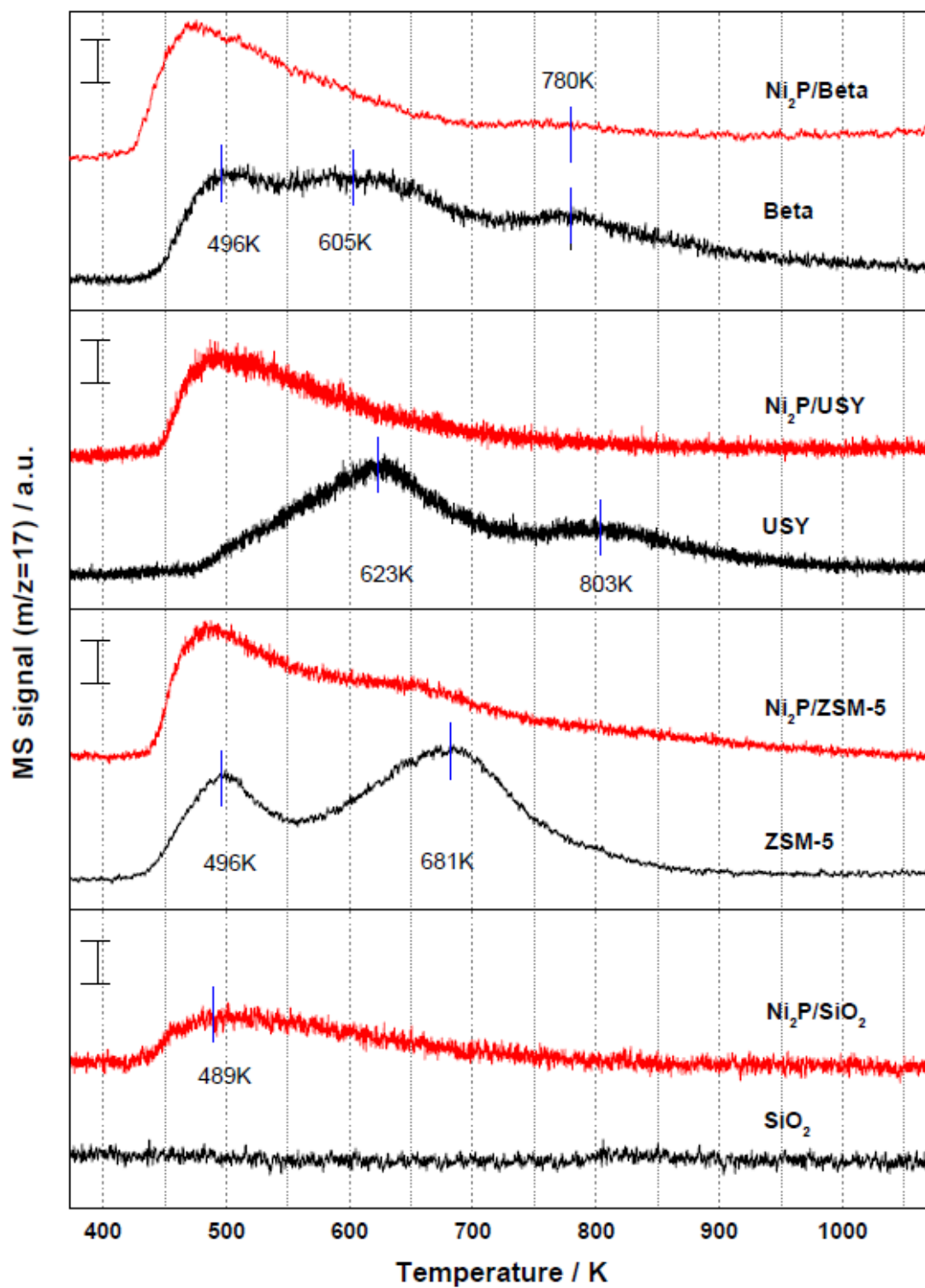
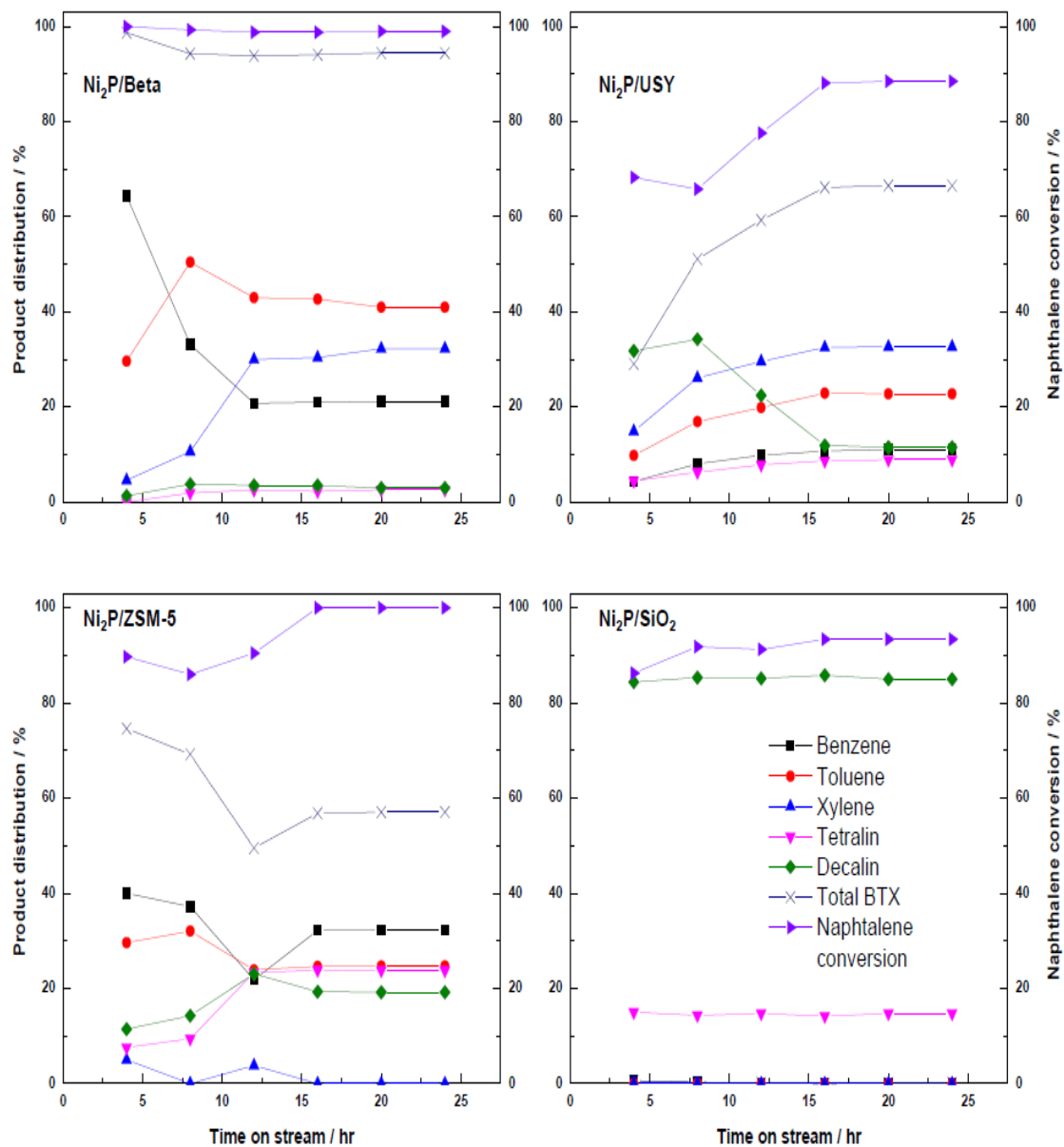
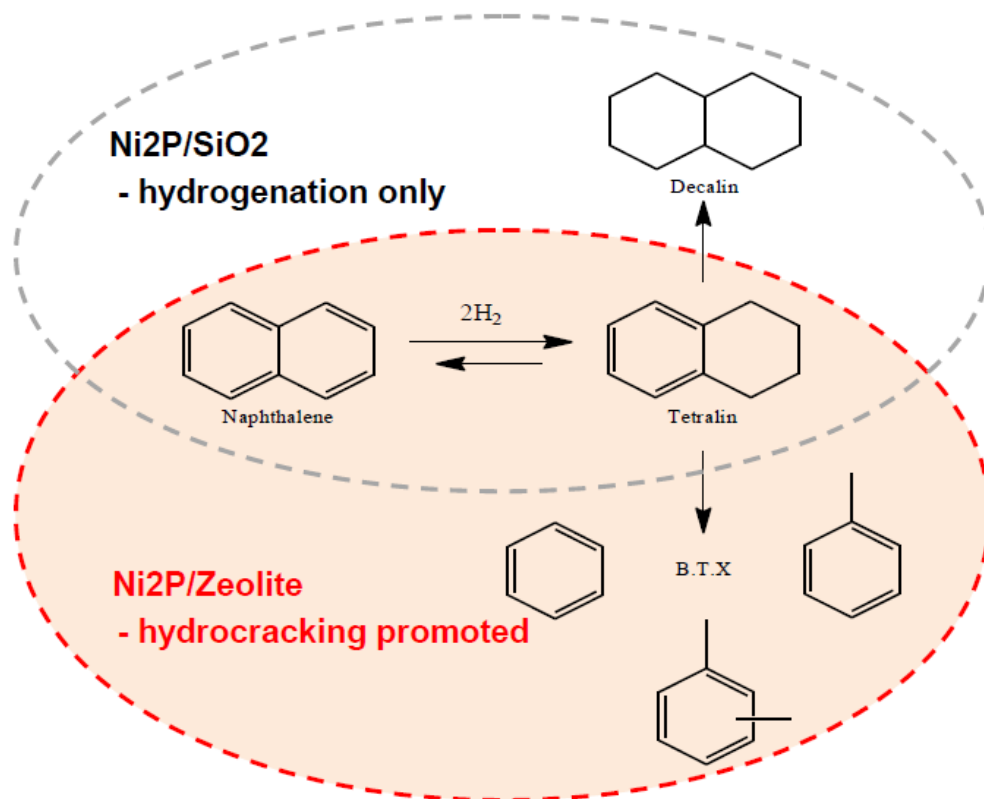


Figure 5



**Graphical abstract**

**Highlights**

- Ni<sub>2</sub>P/zeolite catalysts were active for naphthalene hydrocracking into BTX.
- Ni<sub>2</sub>P/Beta exhibited best activity and selectivity in naphthalene hydrocracking into BTX.
- Bifunctional activity of Ni<sub>2</sub>P/Beta facilitated the hydrocracking of naphthalene.
- Pore structure of zeolite support significantly affected BTX yield.